MICHIGAN STATE UNIVERSITY

CYCLOTRON LABORATORY

MODELS FOR NUCLEAR MATRIX ELEMENTS IN DOUBLE BETA DECAY

Invited talk given by Alex Brown at the Third International Spring Seminar on Nuclear Physics: Understanding the Variety of Nuclear Excitations, Ischia, May 21-25, 1990

B. ALEX BROWN and LIANG ZHAO

JULY 1990

MSUCL-735

MSUCL-735
July, 1990

Models for Nuclear Matrix Elements in Double Beta Decay

B. Alex Brown and Liang Zhao
Cyclotron Laboratory and Department of Physics and Astronomy
Michigan State University, *East Lansing,* Michigan 48824

ABSTRACT

The two-neutrino double-bets ($2\nu\beta\beta$) decay matrix element of ^{48}Ca has been studied in a large-basis shell-model space which explicitly includes approximately 5000 intermediate 1^+ states. The theoretical and experimental β^- and β^+ spectra and their relation to $2\nu\beta\beta$ are discussed. A new empirical shell-model interaction based on a modified-surface one-boson exchange potential is found to give excellent agreement to the observed β^- and β^+ spectra with an effective Gamow-Teller operator which is reduced by a factor of 0.77 from its free-nucleon value. However, the predicted $T_{1/2}$ value of 1.9×10^{19} yr differs by a factor of two from the present experimental upper limit of $T_{1/2} > 3.6\times10^{19}$ yr. We have also investigated to what extent the large-basis results for Gamow-Teller β decay in the fp shell can be reproduced by the QRPA.

1. Introduction

The nuclear shell model has been extensively developed over the past 40 years [1,2]. In many current applications, for all, or a large subset of the nearly degenerate valence configurations, the Hamiltonian can be diagonalized exactly. The spherical shell-model mean field is used as a basis for evaluating the matrix elements of the residual two-body interaction between the valence particles. The wave functions resulting from such calculations can be used to evaluate various quantities of experimental interest. These quantities range from the energies and J^π values which result directly from the Hamiltonian to those which involve expectation values of a few nucleon creation and annihilation operators. The shell-model wave functions provide a general and complete way of relating a wide variety of nuclear data. The use of wave functions which have been successfully tested against conventional observables is important for astrophysical applications and the analysis of fundamental interactions in nuclei such as those involved in isospin nonconservation, parity nonconservation and double-beta decay.

In this paper we will discuss recent calculations for the double-beta decay of ^{48}Ca in the context of an improved interaction and model space for this region. After a few general remarks in this section, we discuss the large-basis calculations for ^{48}Ca in section 2. In section 3 we discuss some comparisons between large-basis shell-

Invited talk given by Alex Brown at the Third International Spring Seminar on Nuclear Physics: Understanding the Variety of Nuclear Excitations, Ischia, May 21-25, 1990.

model results for Gamow-Teller beta decay and those obtained within the QRPA approximation.

For light nuclei (A<50), one is now able to exactly incorporate most of the configurations within the valence oscillator shells. For these cases the improvements in the wave functions are due to the increase in the number of basis states which can be considered and in the development of better effective Hamiltonians. I will discuss results from these type of calculations. For heavy nuclei, the basis truncation is the main problem and there are many competing models. Intermediate mass nuclei such as those in the A=50-80 region provide a place to compare the more exact approach used for light nuclei with the approximations used in heavier nuclei.

The computational aspects have been improved by the introduction of more powerful and more general computer codes [3] as well as by the increase in the speed and disk storage capacity of computers. About 15 years ago the full 1s0d-shell matrix for ^{28}Si which has a dimension of about 6,700 in the J-scheme and 94,000 in the M-scheme was considered "state-of-the-art." Within the last few years one can find in the literature calculations which are almost an order of magnitude larger, e.g. about 62,000 in the J-scheme [4], and 320,000 in the M-scheme [5]. With the continued improvement in codes and computers these dimensions will certainly increase further. Overall, however, most of the advance is made possible by the subsequent ability to carry out faster calculations for the smaller dimensions.

Effective interactions continue to be improved. Wildenthal's USD two-body matrix elements for the 1s0d-shell are perhaps the best example of what can be achieved [6]. Analysis of these matrix elements shows [7] that they are qualitatively (about 80%) what is expected from the microscopic G-matrix approach starting from nucleon-nucleon scattering data. However, fine tuning the remaining 20% is essential to obtain good wave functions for all 1s0d-shell nuclei. The reason for this 20% adjustment is not clear, but there are probably many contributing factors. At the level of the G matrix calculation one should make an interpolation of the G matrix elements between ^{16}O and ^{40}Ca. Also one should use radial wave functions which are more realistic than the harmonic oscillator. (This last point opens up the possibility that one should be using single-particle and two-body matrix elements which are much more mass and state dependent than the smooth dependence usually assumed.) In addition, there may be problems beyond the G-matrix level related to modifications of the nucleon properties in the nuclear medium.

Phenomenologically, the effective interaction appears to be well modeled by the effective two-body matrix element form as used by Wildenthal, or the density-dependent potential form used in Hartree-Fock [8] and shell-model [7] applications. The parameters in these forms should be physically reasonable, and the number of free parameters must be carefully chosen. If the number of parameters is too small, the known data may not be well described. If the number of parameters is too large, the extrapolation is more likely to be incorrect. My current favorite compromise is the "modified surface one-boson exchange potential" (MSOBEP). For the 1s0d-shell, matrix elements obtained from this potential are very similar to Wildenthal's USD matrix elements but has only 17 parameters [7] (compared to Wildenthal's 47).

The ^{48}Ca double-beta decay calculations are based on a successful application of the MSOBEP to the 1p0f shell [9].

2. Large-Basis Shell-Model Calculation for $2\nu\beta\beta$

The study of double-beta decay in nuclei is an area where nuclear physics can add to the understanding of fundamental particles and interactions. Standard two-neutrino double-beta ($2\nu\beta\beta$) decay is a process which should proceed as expected from the second-order weak interaction process. The first laboratory observation of $2\nu\beta\beta$ has recently been reported [10]. Nonstandard zero-neutrino double-beta ($0\nu\beta\beta$) decay is allowed only if the neutrino has a mass; it also depends on the form of the weak interaction currents [11,12]. As of now there are only experimental limits on $0\nu\beta\beta$ decay.

It turns out that the nuclear matrix elements for $\beta\beta$ are very hindered relative to the single-particle estimates and are thus sensitive to nuclear structure considerations. In fact most of the nuclei of interest are in the A=76-100 mass range here the type of large-scale shell-model calculations I have been discussing are very difficult. The most reliable results to date for these nuclei are thought to be obtained from QRPA calculations [13,14,15]. When these QRPA calculations are compared to the experimental limits which exist on $0\nu\beta\beta$ decay, the upper limits on the neutrino mass are in a range of less 2-10 eV [13]. Further improvements in the experimental limits may be able to push this limit down to the range of a few tenth of keV. This is also consistent with the 27 eV upper limit obtained in the Los Alamos tritium decay experiment [16], although inconsistent with the Russian result [17]. Even though there is only an outside chance that the neutrino mass is in the range of 0.1 to 10 keV, it is important to continue to improve the experimental and theoretical analysis.

Here we discuss some new calculations for the $\beta\beta$ decay of ^{48}Ca [18]. Although ^{48}Ca has the largest $\beta\beta$ Q-value [11], it has not been as well studied as some of the heavier nuclei. Experimentally this is because the ^{48}Ca source is not easy to obtain or handle. Theoretically the $\beta\beta$ matrix elements are thought to be particularly hindered. However, ^{48}Ca is interesting because it can be calculated in a much more complete basis than is possible for the heavier nuclei.

We have calculated the $2\nu\beta\beta$ decay in much larger model space than previously used and with a new interaction which we test by comparing with the β^+ and β^- spectra obtained from recent ^{48}Ti(n,p) and ^{48}Ca(p,n) experiments. In previous calculations where the intermediate 1^+ states have been considered explicitly, the 1p0f shell model space was highly truncated [19,20,21], and in other cases where the truncation was not so severe, the closure approximation was used [11,22]. Most recently, Horie and Ogawa carried out the $2\nu\beta\beta$ in the full 1p0f model space but with a new method that does not require an explicit spectrum of intermediate 1^+ states [4].

Our calculations were carried out in the truncation defined by $0f_{7/2}^{8-r}(1p_{3/2}, 0f_{5/2}, 1p_{1/2})^r$ where $r\leq 4$ for the 0^+ ground states of ^{48}Ca and ^{48}Ti and $r\leq 5$ for the

1^+ states in ^{48}Sc. In this truncation there are 5599 1^+, T=3 states in ^{48}Sc. The $2\nu\beta\beta$ matrix element obtained in this truncation is within a few percent of the one obtained by Horie and Ogawa [4] in the full 1p0f model space ($r \leq 8$) with the same interaction. Additional comparisons of truncated and full space calculations for the $2\nu\beta\beta$ matrix element for ^{46}Ca and 1s0d-shell nuclei, lead us to conclude that our truncation gives results for the ^{48}Ca $\beta\beta$ decay which are essentially the same as those that would be obtained in the full 1p0f model space.

We have compared the results obtained with two interactions. One (which we label by MH) was used by Tsuboi, Muto and Horie in a very truncated calculation ($r \leq 2$) [19] and then by Horie and Ogawa in the full space calculation [4]. The MH interaction has a long history. McGrory et al. [23] started with the renormalized Kuo-Brown interaction and changed several T=1 two-body matrix elements which involved the $0f_{7/2}$ and/or $1p_{3/2}$ orbits. Later McGrory et al. [24] added 50 keV to the $0f_{7/2}$-$0f_{5/2}$ diagonal T=1 matrix elements and introduced new single-particle energies. Based on Ref 23, Muto and Horie [25] shifted the monopole part of the inter-shell T=0 matrix elements $<0f_{7/2},j|V|0f_{7/2},j>$ ($j=1p_{3/2},1p_{1/2},0f_{5/2}$) by -0.3 MeV.

Our new interaction labeled MSOBEP is based on the modified surface one-boson exchange potential [7]. Parameters of this potential have been determined by a fit to 61 energy level and binding energy data for nuclei in the lower part ($A<48$) of the 1p0f shell [9]. The parameters varied were six strengths associated with the central part of the potential and the four single-particle energies. The parameters associated with the spin-orbit and tensor parts of the potential were kept fixed at the values obtained in the 1s0d shell [7]. The rms deviation between experiment and theory was 176 keV.

The effects of higher-order configuration mixing outside the 1p0f shell and mesonic exchange currents (including Δ-isobar nucleon-hole configurations) were taken into account by using the effective Gamow-Teller operator given by $\sigma t^-(\mathrm{eff}) = 0.77\sigma t^-$. This renormalized form of the effective operator is empirically well established from beta decay data in the 1s0d shell [26] and 1p0f shell [27,28]. Also, the contributions of these effects to the interaction are presumably taken into account by the adjustments of the potential parameters to fit experimental binding energies. The direct contribution of the Δ-isobar nucleon-hole configurations on the $\beta\beta$ decay is negligible because of the large energy denominator and because of cancellations between β^+ and β^- [22,29]. We believe that the direct contribution of the higher-order configuration mixing on the $\beta\beta$ matrix element is small, but should be further investigated.

We write the $2\nu\beta\beta$ matrix element as

$$M_{GT}(E_m) = \Sigma_{m=1}^{E_m} <0_f^+ \,||\, \sigma t^-(\mathrm{eff})||1_m^+ > <1_m^+ \,||\, \sigma t^-(\mathrm{eff})||0_i^+ > / \,(E_m+E_o)$$

where $E_o = (T_o/2)+\Delta M$, T_o is the $\beta\beta$ Q-value (4.27 MeV), ΔM is the mass difference between ^{48}Sc and ^{48}Ca (-0.277 MeV), and E_m is the excitation energy of the 1_m^+ state in ^{48}Sc. The total $2\nu\beta\beta$ matrix element is given by $M_{GT}^{2\nu}=M_{GT}(E_m=\infty)$. The Fermi

contribution vanishes when isospin is conserved and an estimate of its contribution with isospin-mixed wave functions indicates that it can be neglected [20]. The half-life is given by

$$(1/T_{1/2}) = G\ |M^{2\nu}_{GT}\ |^2$$

where G is related to the fundamental constants and phase space integrals which depend somewhat on the intermediate state strength distribution [19]. We use a value of G=1.10x10^{-17} yr^{-1} (MeV)^2 deduced from the first row in Table 1 of Ref 19.

The individual matrix in the expression for $M_{GT}(E_m)$ can be studied with in the ^{48}Ti(n,p) and ^{48}Ca(p,n) reactions. In Fig. 1 I show the B(GT$^-$) = $|<1^+_m\ ||\ \sigma t^-(\text{eff})\ ||0^+_i>|^2$ values for the ^{48}Ca $\rightarrow$ ^{48}Sc transitions as a function of excitation energy. Since there are several hundred 1^+ states calculated to be in the region between 5 and 15 MeV excitation, the B(GT) values have been smoothed by folding with a Gaussian function. The bottom curve is the GT distribution extracted from the peaks above the background in the experimental cross section at 0° [27]. The middle spectra show the calculations for the GT distribution for the MH (dotted curve) and MSOBEP (solid curve) interactions with a 400 keV full width at half maximum (FWHM) smoothing chosen to match the experimental resolution. (The top curve shows the MSOBEP results with 100 keV FWHM to show what the ideal experiment might look like.) The results with the MSOBEP interaction are in best agreement with experiment. The apparent overestimation of strength in the region around 10 MeV in excitation energy is resolved by including the extra strength extracted from the background spectrum. It is interesting to note that the lowest 1^+ state obtained with the MH interaction does not have the predominant $(\nu 0f_{7/2})^{-1}(\pi 0f_{7/2})^1$ structure expected from experiment. Rather, this interaction pulls down another configuration which appears to have a ^{46}Ca + deuteron cluster structure as its dominant configuration. Thus the "particle-particle" part of the MH interaction appears to be slightly too strong.

In Fig. 2 I show the B(GT$^+$)=$|<0^+_f\ ||\ \sigma t^-(\text{eff})\ ||1^+_m>|^2$ values for the ^{48}Ti $\rightarrow$ ^{48}Sc transitions as a function of excitation energy. In this case each B(GT) value is shown by an isolated peak. The bottom curve shows the values deduced by a fit of the experimental (n,p) spectrum [30] to peaks centered at the known location of 1^+ states. Comparison with the calculations again shows that the MSOBEP results (middle spectrum) are in better agreement with experiment than the MH results (top spectrum).

These comparisons show the importance of being able to explicitly calculate the spectra of the intermediate 1^+ states and the importance of having experimental data for both the β^- and β^+ directions. The individual β^+ and β^- matrix elements can now be combined to form the $2\nu\beta\beta$ matrix element. In Fig. 3 I show $M_{GT}(E_m)$ as a function of E_m for the MH (dotted line) and MSOBEP (solid line) interactions. The general feature of these curves is similar to what has been found in an earlier more truncated calculation [19], namely, a quick rise from the first few states, followed

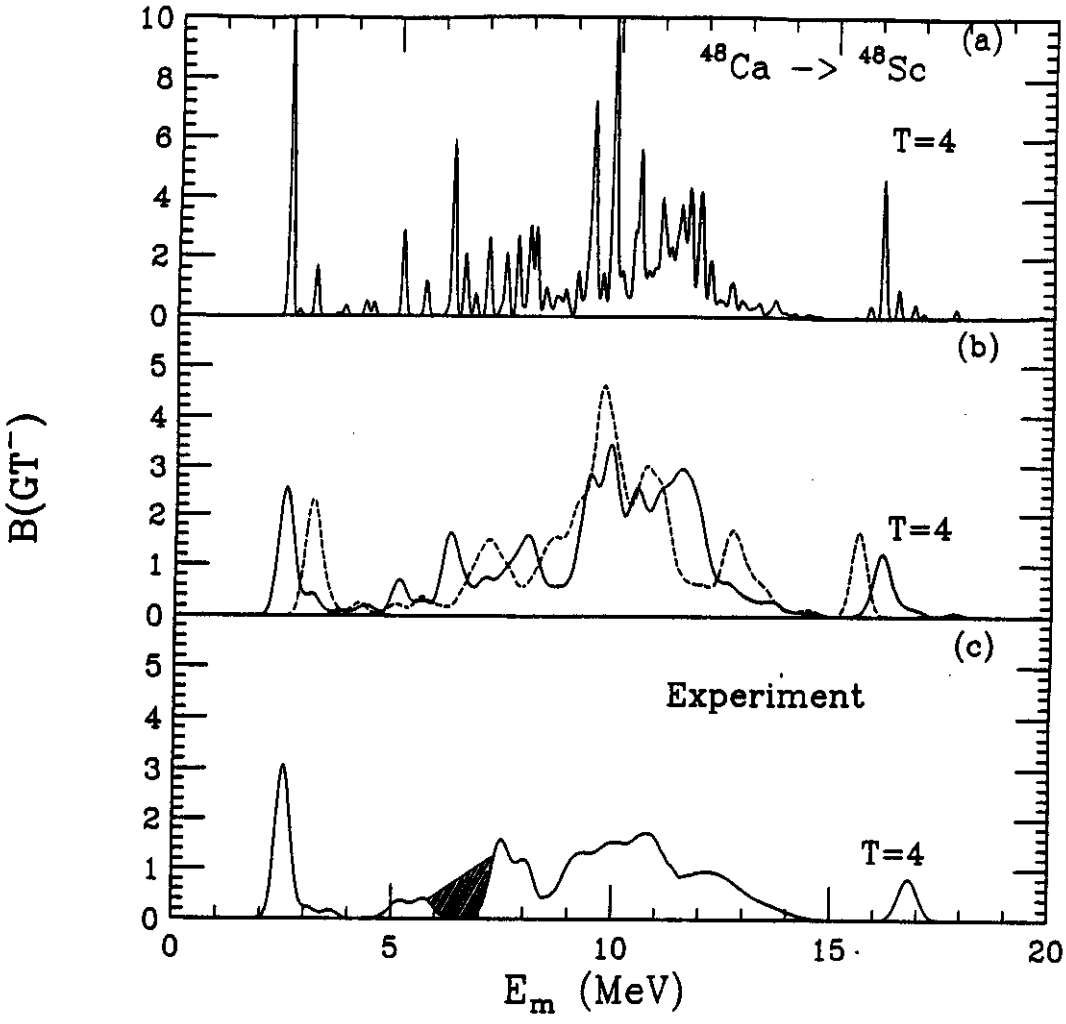

Figure 1: B(GT^-) values for $^{48}Ca \rightarrow {}^{48}Sc$ as a function of E_m. The bottom curve is the GT distribution extracted from the peaks above the background in the experimental (p,n) cross section at 0^o [27]. The shaded area indicates the region where the Fermi transition to the 0^+ state has been subtracted. The theoretical curves are obtained by averaging the B(GT) values for individual states over a Gaussian distribution. The middle spectra for the MH (dashed line) and MSOBEP (solid line) interactions were obtained with FWHM=400keV. The top spectrum for the MSOBEP interaction was obtained with FWHM=100keV.

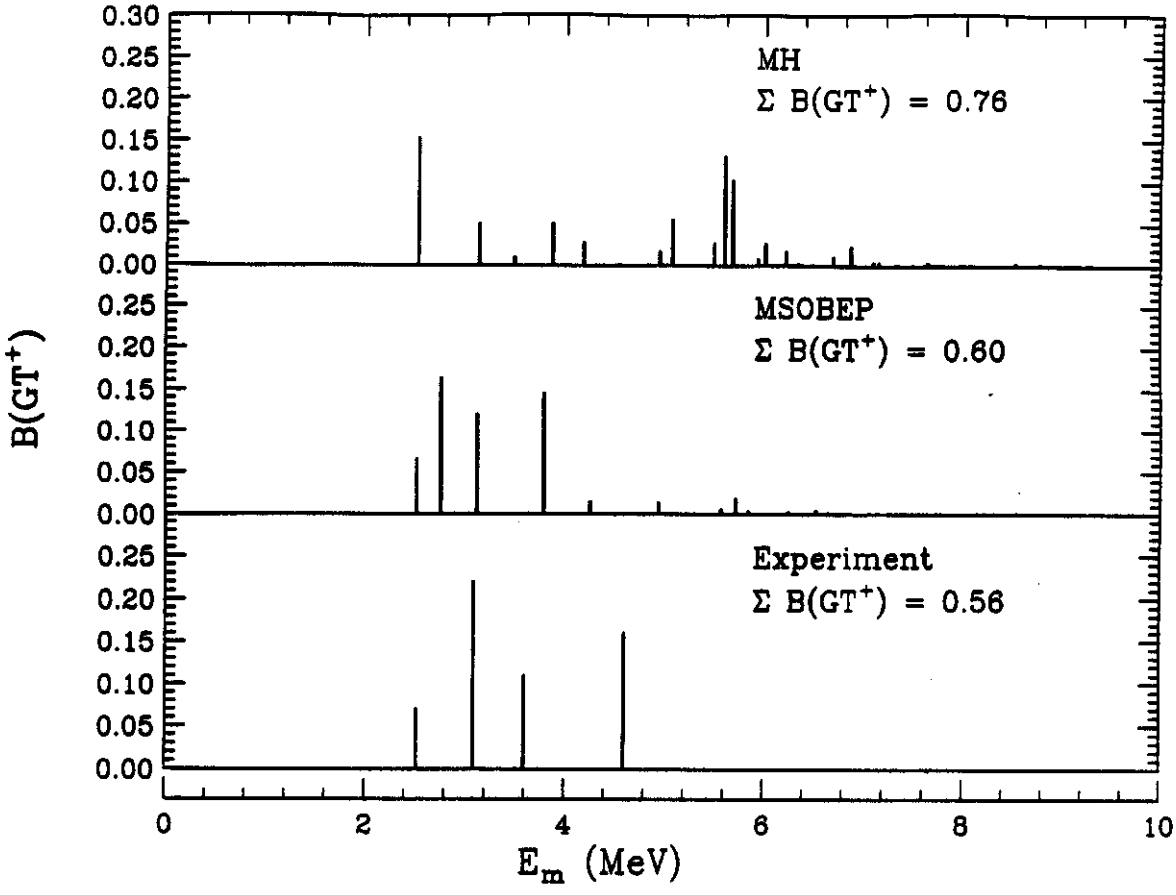

Figure 2: $B(GT^+)$ values for $^{48}Ti \rightarrow {}^{48}Sc$ as a function of E_m. Each B(GT) value is indicated by an isolated peak. The bottom curve shows the values deduced by a fit of the experimental (n,p) spectrum [30] to peaks centered at the known location of 1^+ states.

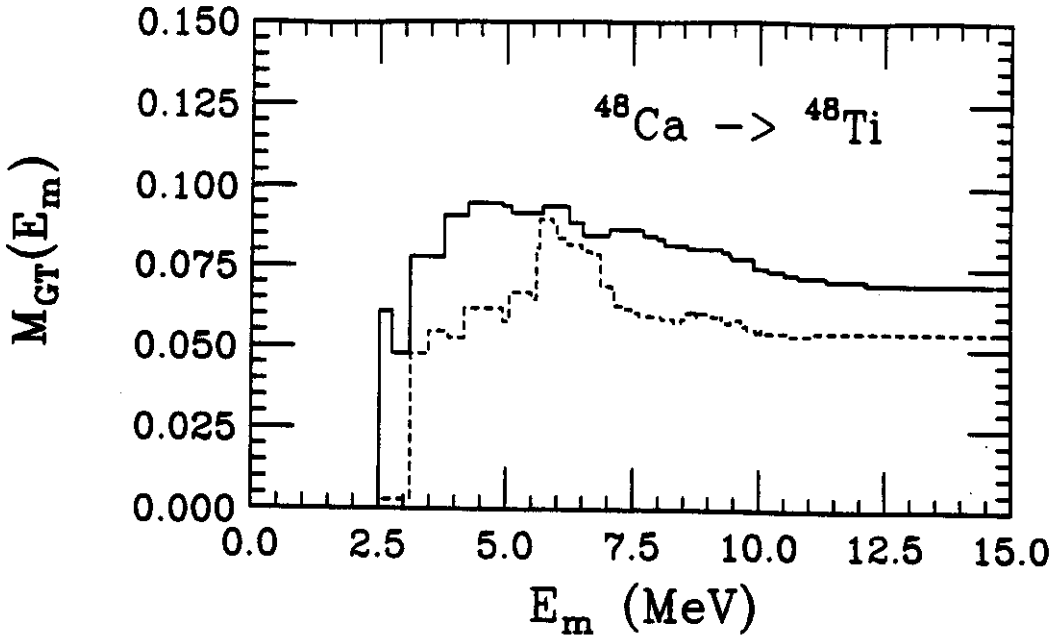

Figure 3: The $2\nu\beta\beta$ matrix element $M_{GT}(E_m)$ as a function of E_m. The solid line corresponds to the results with the MSOBEP interaction and the dashed line corresponds to those for the MH interaction.

by a more gradual rise from the states up to about 6 MeV in excitation, followed by a fall off (cancellation) from the remaining states up to about 10 MeV in excitation. The qualitative nuclear structure reasons for this pattern is discussed in [20,18]. It is remarkable that the total matrix element in the MSOBEP calculation (0.070) is very close to the contribution from the first state alone (0.061).

The value of $M^{2\nu}_{GT}$=0.070 $(MeV)^{-1}$ obtained with the MSOBEP interaction translates into a $2\nu\beta\beta$ $T_{1/2}$ value of 1.9×10^{19}yr compared to the experimental lower limit of $>3.6\times10^{19}$yr [31]. This disagreement between theory and experiment is a puzzle. It turns out that the MH interaction gives a result of 3.0×10^{19}yr which is in better agreement with experiment. However, we have shown above that the MH interaction does not reproduce the β^- and β^+ spectra. It may be that the $2\nu\beta\beta$ matrix element is sensitive to further refinements in the interaction and to the direct effects of the higher-order configuration mixing which do not show up in the β^- and β^+ comparisons made above. In particular, we note that there is a large uncertainty in the Gamow-Teller strength extracted from the (n,p) spectrum above 5 MeV in excitation energy [30]. In any case, it is remarkable that the best calculations and the experimental limit agree with each other within a factor of two out of many possible orders of magnitude, and we hope to encourage further experimental efforts on the ^{48}Ca decay. Calculations for the $0\nu\beta\beta$ matrix elements are in progress. An estimate from previous calculations [20] compared to the experimental lower limit of $T_{1/2}(0\nu\beta\beta)>200\times10^{19}$yr [31] gives an upper limit of about 20 eV for the neutrino mass.

The $0\nu\beta\beta$ matrix element for ^{48}Ca turns out to be less sensitive to the truncation that the $2\nu\beta\beta$ matrix element [20].

3. Comparison with the QRPA Approximation

Most of the interesting cases for $\beta\beta$ decay (^{76}Ge, ^{82}Se, ^{100}Mo, etc.) are in the "transitional" regions between spherical and deformed shapes and are thus particularly difficult to describe theoretically. Shell-model calculations of the type discussed above for ^{48}Ca must be highly truncated, and those that have been carried out [11] can be criticized for omitting some configurations involving the strong mixing between spin-orbit partners. The QRPA has been the most widely used method for calculating the $\beta\beta$ matrix elements in these heavier nuclei [13,14,15]. It is important to test the approximations which go into the QRPA by comparing the results with more exact calculations where possible. Here we use the ^{48}Ti $\rightarrow$ ^{48}Sc β^+ transitions for such a comparison.

The type of comparisons presented here follow along the lines of Lauritzen for β^+ matrix elements in the 1s0d shell [32] and Liang and Brown for β^+ and $\beta\beta$ matrix elements in the 1s0d shell [33]. These studies have focused mainly on the inadequacies of the BCS input to the QRPA equations. One can criticize the generality of the conclusions drawn from the 1s0d-shell comparisons because the validity of the BCS approximation depends on having a large identical-particle level degeneracy. This degeneracy is relatively small in the 1s0d shell compared with the situations in heavier nuclei. Our 1p0f-shell comparisons may be more appropriate in this regard, although there is still some problem with the relative isolation of the $0f_{7/2}$ orbital from the other 1p0f orbitals. From these and other comparisons of this type, the 1p0f shell can serve as a bridge for testing the approximations used in heavy nuclei.

We give the basic equations of QRPA in order to emphasis their dependence on the basic shell-model inputs. The A and B amplitudes in the QRPA matrix are given by [34]

$$\begin{aligned} A(J,pn,p'n') &= g_{ph}\, W(J,pn,p'n')\, (u_p\, v_n\, u_{p'}\, v_{n'} + v_p\, u_n\, v_{p'}\, u_{n'}) \\ &+ g_{pp}\, V(J,pn,p'n')\, (u_p\, u_n\, u_{p'}\, u_{n'} + v_p\, v_n\, v_{p'}\, v_{n'}) + (E_p+E_n)\delta_{pp'}\delta_{nn'} \qquad (1) \end{aligned}$$

$$\begin{aligned} B(J,pn,p'n') &= g_{ph}\, W(J,pn,p'n')\, (v_p\, u_n\, u_{p'}\, v_{n'} + u_p\, v_n\, v_{p'}\, u_{n'}) \\ &- g_{pp}\, V(J,pn,p'n')\, (u_p\, u_n\, v_{p'}\, v_{n'} + v_p\, v_n\, u_{p'}\, u_{n'}) \qquad (2) \end{aligned}$$

The subscripts p and n are the labels for the proton and neutron orbitals, respectively. The v^2 are the quasi-particle occupation probabilities, and E are the quasi-particle energies. V are the MSOBEP two-body matrix elements discussed in the last section expressed in the proton-neutron basis, and W are the particle-hole Pandya

transform of these:

$$W(J,pn,p'n') = -(-1)^{j_p+j_n+j_{p'}+j_{n'}} \Sigma_{J'}(2J'+1)\, R(j_p j_n j_{n'} j_{p'};JJ') \times V(J',pn,p'n') \quad (3)$$

where R(;) is the Racah coefficient. The multiplicative factors g_{ph} (particle-hole) and g_{pp} (particle-particle) are conventionally introduced in order to discuss the results as a function of the strength associated with each part of the interaction. The matrix elements discussed here are more sensitive to g_{pp} than to g_{ph}, and in the following will set $g_{ph} = 1$ and discuss the dependence on g_{pp}.

The occupation factors u and v and quasi-particle energies E can be obtained from the from the BSC equations

$$E_p = [(e_p-\lambda_\pi)^2 + \Delta_p^2]^{1/2} \quad (4)$$

$$2v_p^2 = 1 - (e_p-\lambda_\pi)/\,[\,(e_p-\lambda_\pi)^2 + \Delta_p^2\,]^{1/2} \quad (5)$$

$$v_p^2 + u_p^2 = 1 \quad (6)$$

$$2\Delta_p = -(2j_p+1)^{-1/2} \Sigma_{p'}\, (2j_{p'}+1)^{1/2}\, V(J=0,pp,p'p')\, u_{p'}\, v_{p'} \quad (7)$$

where, again, the subscript p is the label for the proton orbital. The e_p are the effective single-particle energies. Given e_p and the two-body matrix elements, these equations can be solved under the constraint for the total number of protons N_π:

$$N_\pi = \Sigma_p\, (2j_p+1)\, v_p^2 \quad (8)$$

which determines the constant λ_π. A similar set of equations can be solved for the neutrons. The effective single-particle energies e_p are related to the bare single-particle energies ϵ_p at ^{40}Ca by the addition of the rearrangement term Γ_p:

$$e_p = \epsilon_p + \Gamma_p \quad (9)$$

where

$$\Gamma_p = (2j_p+1)^{-1} \Sigma_{p'}\, (1+\delta_{p,p'})\, v_{p'}^2\, \Sigma_J\, (2J+1)\, V(J,pp',pp') + (2j_p+1)^{-1} \Sigma_{n'}\, v_{n'}^2\, \Sigma_J\, (2J+1)\, V(J,pn',pn') \quad (10)$$

The rearrangement term for e_n has the same form but with the p/n indices inter-

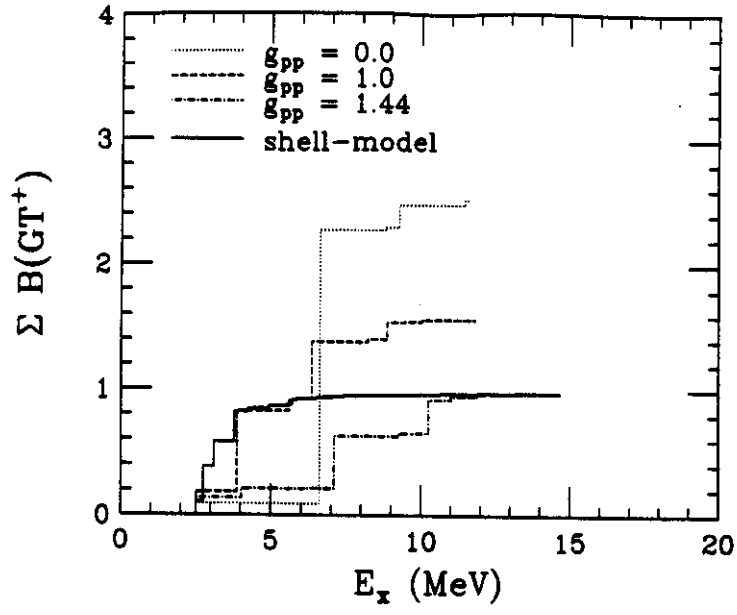

Figure 4: Running sum of the B(GT$^+$) values for ^{48}Ti → ^{48}Sc as a function of E_x. The large-basis shell-model result (solid line) is compared to the QRPA results obtained with various values of g_{pp} (g_{ph}=1).

changes. The BCS equations plus the rearrangement terms can easily be solved iteratively.

Thus we have defined the precise ingredients of a QRPA calculation in which the input is exactly the same as a shell-model calculation, namely, the bare single-particle energies ϵ_i and the two-body matrix elements V(J,ij,kl). In practice, when the QRPA equations are used in heavier nuclei, u, v and E are often not obtained in this way but are based on some empirical value for the pairing gap Δ (often one which is orbit independent) and on some interpolated values for the the effective single-particle energies.

We will now compare the QRPA results for the ^{48}Ti → ^{48}Sc B(GT$^+$) spectrum with those discussed in section 2 based on the large-basis shell-model calculation. We show in Fig. 4, the running sum of the B(GT$^+$) values as a function of excitation energy E_x in ^{48}Sc. The shell-model results are shown by the solid line. This is compared with the QRPA results obtained with three different values of g_{pp} (g_{ph}=1). The results obtained from the nominal value of g_{pp}=1 (dashed line) look reasonable up to 5 MeV and then overshoot the shell-model by about 50%. If we adjust g_{pp} to get agreement with the total B(GT$^+$) strength (a procedure which is often used in the application of QRPA to heavy nuclei) then the strength distribution is in very poor agreement with the shell-model.

We are investigating various ways to understand and then improve the disagreement between QRPA and the shell-model [35]. Here we will just show one inter-

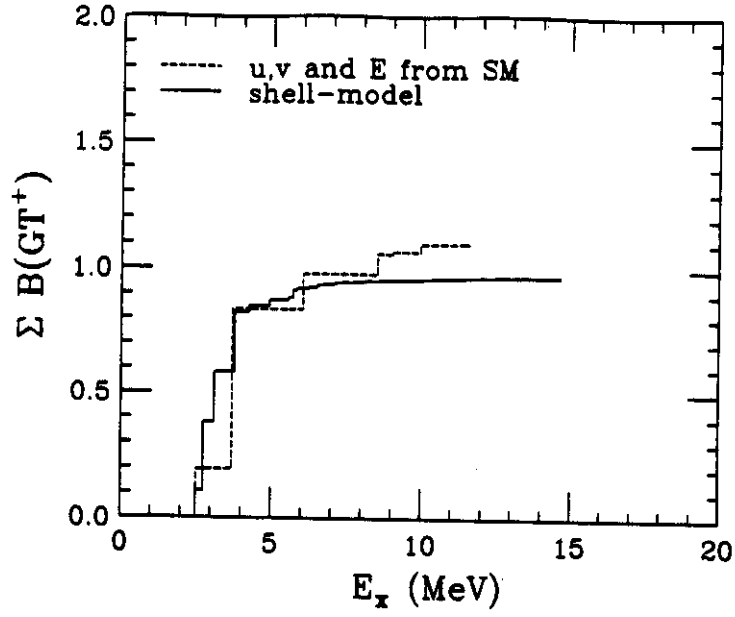

Figure 5: Running sum of the B(GT$^+$) values for ^{48}Ti → ^{48}Sc as a function of E_x. The large-basis shell-model result (solid line) is compared to the QRPA calculation with the u,v and E factors taken from the shell-model calculations as described in the text.

esting result. We can replace the BCS occupation factors in the QRPA equations with those obtained from the shell-model ground-state wave function of ^{48}Ti and replace the BCS quasi-particle energies with those obtained by the shell-model calculations for the Ca isotopes. As shown in Fig. 5, the results from this modified QRPA calculations is now in better agreement with the full shell-model calculation. Thus, it may be possible to put together "hybrid" models of this type that are more reliable than the conventional QRPA. It is difficult to extend this comparison to the ^{48}Ca $\beta\beta$ matrix element because of the semi-closed shell nature of ^{48}Ca and the problem of matching the QRPA spectra from two different ground states. More work remains to be done to arrive at some definitive conclusions concerning the adequacy of the QRPA approach to $\beta\beta$ matrix elements.

4. Acknowledgements

We wish to thank Ahmad Ansari for helpful discussions concerning the BCS calculations. This work was supported in part by the US National Science Foundation grant number PHY-87-14432.

5. References

1. B. A. Brown, in The Nuclear Shell Model, edited by T. -S. H. Lee and R. B.

Wiringa, (North Holland, Amsterdam, 1990).

2. B. A. Brown and B. H. Wildenthal, Ann. Rev. of Nucl. and Part. Sci. 38 (1988) 29.

3. B. A. Brown, in Workshop on Microscopic Models in Nuclear Structure Physics, edited by M. W. Guidry, J. H. Hamilton, D. H. Feng, N. R. Johnson and J. B. McGrory (World Scientific, singapore, 1989) p. 337.

4. K. Ogawa and H. Horie, in Nuclear Weak Process and Nuclear Structure, edited by M. Morita, H. Ejiri, H. Ohtsubo and T. Sato, (World Scientific, Singapore, 1989) p. 308.

5. J. A. Carr et al., Phys. Rev. Lett. 62 (1989) 2249.

6. B. H. Wildenthal, Progress in Particle and Nuclear Physics 11 (1984) 5.

7. B. A. Brown, W. A. Richter, R. E. Julies and B. H. Wildenthal, Ann. Phys. 182 (1988) 191.

8. J. Decharge and D. Gogny, Phys. Rev. C33 (1986) 335.

9. W. A. Richter, R. E. Julies and B. A. Brown, unpublished.

10. S. R. Elliott, A. A. Hahn and M. K. Moe, Phys. Rev. Lett. 59 (1987) 2020.

11. W. C. Haxton and G. J. Stephenson, Prog. in Part. and Nucl. Phys. 12 (1984) 409.

12. M. Doi et al., Prog. Theor. Phys. Suppl. 83 (1985) 1.

13. K. Muto, E. Bender and H. V. Klapdor, Z. Phys. 334 (1989) 177; 334 (1989) 187.

14. T. Tomoda and A. Faessler, Phys. Lett. 199B (1987) 475.

15. J. Engel, P. Vogel and M. R. Zirnbauer, Phys. Rev. C37 (1988) 731.

16. J. F. Wilkerson et al., Phys. Rev. Lett. 58 (1987) 2023.

17. S. Boris et al., Phys. Rev. Lett. 58 (1987) 2019.

18. L. Zhao and B. A. Brown, Phys. Rev. C, to be published.

19. T. Tsuboi, K. Muto and H. Horie, Phys. Lett. 143B (1984) 293.

20. B. A. Brown, in Nuclear Shell Models, edited by M. Vallieres, and B. H. Wildenthal, (World Scientific, Singapore, 1985), p. 42.

21. L. D. Skouras and J. D. Vergados, Phys. Rev. C28 (1983) 2122; J. D. Vergados, Phys. Rep. 133 (1986) 1.

22. L. Zamick and N. Auerbach, Phys. Rev. C26 (1982) 2185.

23. J. B. McGrory, B. H. Wildenthal and E. C. Halbert, Phys. Rev. C2 (1970) 186.

24. J. B. McGrory and B. H. Wildenthal, Phys. Lett. 103B (1981) 173.

25. K. Muto and H. Horie, Phys. Lett. 138B (1984) 9.

26. B. A. Brown and B. H. Wildenthal, At. Data and Nucl. Data Tables 33 (1985) 347.

27. B. D. Anderson et al. Phys. Rev. C31 (1985) 1161, and private communication.

28. J. Rapaport et al., Nucl. Phys. A427 (1984) 332.

29. K. Grotz and H. V. Klapdor, Nucl. Phys. A460 (1986) 395.

30. W. P. Alford et al., to be published in Nucl. Phys. A.

31. R. K. Bardin et al., Nucl. Phys. A158 (1970) 337.

32. B. Lauritzen, Nucl. Phys. A489 (1988) 487.

33. B. A. Brown and L. Zhao, in Nuclear Weak Process and Nuclear Structure, edited by M. Morita, H. Ejiri, H. Ohtsubo and T. Sato, (World Scientific, Singapore, 1989) p. 291.

34. D. Cha, Phys. Rev. C27 (1983) 2269.

35. L. Zhao and B. A. Brown, unpublished.